# Chapter 3
# Efficiency Limits for Solar Spectrum Rectification

**Saumil Joshi, Sachit Grover, and Garret Moddel**

**Abstract** Optical rectennas are antennas coupled to high-speed diodes used to convert high-frequency optical radiation to DC. Rectennas have been viewed as alternatives to conventional p-n junction solar cells, with the potential of exceeding the Shockley-Queisser conversion efficiency limit of 33 %. Using the theory of photon-assisted tunneling, we analyze the efficiency limits and show that rectennas can achieve efficiencies up to 100 % under monochromatic illumination. For broadband solar illumination, we find that the diode operating voltage plays the role that bandgap plays in conventional solar cells. We study the effects of poor antenna/diode matching and diode reverse leakage currents showing the importance of careful diode design. We highlight the correspondence between rectification in the classical and quantum limits.

## 3.1 Introduction

The concept of a rectenna, a rectifying antenna, was developed in the early 1960s at Raytheon to power heavier-than-air vehicles, effectively demonstrating power transfer at microwave frequencies. These first rectennas used half-wave dipole antennas and point-contact diodes as receivers and rectifying elements and had greater than 70 % power conversion efficiency for low-frequency monochromatic radiation [1]. The use of rectennas as solar cells emerged in 1971 when Bailey suggested solar energy converters exploiting the wave nature of light [2] instead of

S. Joshi • G. Moddel (✉)
Department of Electrical, Computer, and Energy Engineering,
University of Colorado, Boulder, CO 80309-0425, USA
e-mail: moddel@colorado.edu

S. Grover
National Center for Photovoltaics, National Renewable Energy Laboratory,
15013 Denver West Parkway, Golden, CO 80309-0425, USA

G. Moddel and S. Grover (eds.), *Rectenna Solar Cells*,
DOI 10.1007/978-1-4614-3716-1_3, 

the conventional photon approach employed by semiconductors. Concurrently, high-frequency diodes were being developed for applications such as terahertz detection and mixing using metal-insulator-metal (MIM) diodes and cat's whisker diodes [3]. Bailey's proposition was seen as a concept that could overcome the Shockley-Queisser efficiency limit faced by single junction solar cells [4]. The fact that microwave rectennas could approach very high efficiencies [5], coupled with the 93 % thermodynamic limit of using solar blackbody radiation [6], is promising. Significant effort has been put into studying the diode limitations [7], improving the characteristics and extending the operating frequency of MIM diodes [8–11] using novel concepts to the visible portion of the electromagnetic spectrum for use as solar energy harvesters [12, 13]. A generalized theory of rectenna rectification of a broadband spectrum is required to explain and predict diode behavior at optical frequencies.

Limited work has been done to study rectenna operation and efficiency limits. Existing research is based on a general framework of employing thermodynamic concepts and to study rectifier efficiency [14]. These approaches, although important, tell little about the rectenna design issues. The work of Shockley and Queisser [4] is specific to p-n junction solar cells. Classical analysis of rectennas with MIM diodes [15] is insightful but cannot be applied at high frequencies. Some important rectenna efficiency issues from thermodynamic considerations are reviewed in [16]. The results given in this chapter are an elaboration of recently published work [17, 18].

In this chapter, we study the efficiency limits of optical rectennas using the theory of photon-assisted tunneling (PAT) developed by Tien and Gordon, which is analyzed in detail in Chap. 2 and described briefly in Sect. 3.2. In Sect. 3.3, the rectenna efficiency limits for the case of monochromatic, dichromatic, and multispectral illumination will be discussed. We will show that rectennas can achieve efficiencies approaching 100 % under monochromatic illumination. For broadband illumination, rectennas can achieve an efficiency limit potentially higher than the Shockley-Queisser limit for conventional solar cells. The performance resulting from nonideal diodes is discussed in Sect. 3.4. In Sect. 3.5, we will develop the correspondence between the classical low-frequency and semiclassical high-frequency rectification. This chapter focuses on calculating the fundamental efficiency limits of rectennas. We do not investigate antenna efficiency limits, which are assumed to be ideal.

## 3.2 Theory

Rectenna operation is a function of the incident radiation, the antenna, and the diode. The antenna receives the high-frequency electromagnetic radiation and couples the power to the diode. The antenna impedance and the diode current–voltage [$I(V)$] characteristics determine the coupling efficiency. In this section, we use the theory of PAT to explain diode behavior, describe the rectenna circuit model, and develop the diode $I(V)$ characteristics for optimum antenna/diode coupling.

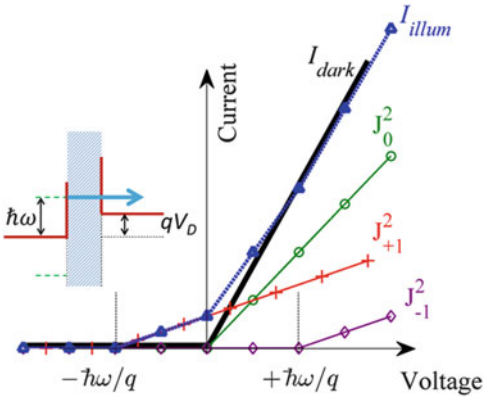


**Fig. 3.1** Illustration of photon-assisted tunneling (PAT) for a diode having a piecewise linear $I(V)$ characteristics (*solid curve*). The frequency of the incident photon is $\omega$. Tunneling currents due to photon absorption and emission events are represented by the *pluses* and the *diamonds*, respectively. The *triangles* represent the net DC tunneling current through the diode due to illumination. Under rectenna illumination, the diode generates power in the second quadrant. *Inset* shows the energy diagram of a typical metal-insulator-metal diode. The *dotted horizontal lines* represent the absorption and emission states at energies $\hbar\omega$ above and below the Fermi level. Reprinted with permission [17]. Copyright 2013, American Institute of Physics

### 3.2.1 Photon-Assisted Tunneling

The theory of PAT was developed in 1963 [19] to explain the interaction of microwave radiation with superconductor-insulator-superconductor (SIS) junctions [20]. The theory is suitable to explain the behavior of nonlinear diodes, such as SIS junctions and MIM diodes, under illumination [21]. When the photon energy divided by the electron charge ($\hbar\omega/q$) is comparable to the voltage scale of the nonlinearity in the diode $I(V)$ characteristics, a quantum approach is required to explain diode operation. High-frequency alternating voltage with amplitude of $V_\omega$ gives rise to multiple photon absorption and emission states above and below the metal Fermi energy level. Photon absorption leads to tunneling currents below the knee of the $I(V)$ characteristics (see Sect. 2.4). The resulting $I(V)$ characteristic is illustrated in Fig. 3.1. The rectenna operates in the second quadrant, generating power. The illuminated DC tunneling current is given by the following equation, (3.1):

$$I_{\text{illum}} = \sum_{n=-\infty}^{\infty} J_n^2\left(\frac{qV_\omega}{\hbar\omega}\right) \times I_{\text{dark}}\left(V_{\text{D}} + n\frac{\hbar\omega}{q}\right) \tag{3.1}$$

The $I_{\text{illum}}$ is the DC current under illumination; incident photon energy is $\hbar\omega$, $V_\omega$ is the amplitude of the alternating voltage across the diode, $V_{\text{D}}$ is the DC operating

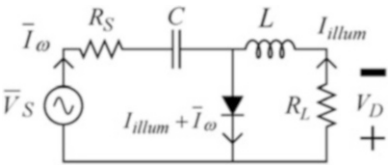


**Fig. 3.2** Equivalent circuit of the rectenna consists of an alternating voltage source $V_S$, antenna impedance $R_S$, a DC current blocking capacitor $C$, large inductor $L$, and a load resistor $R_L$. The inductor $L$ allows only DC power dissipation in the load. Both alternating currents ($I_\omega$) and direct currents ($I_{illum}$) flow through the diode. Reprinted with permission [17]. Copyright 2013, American Institute of Physics

voltage, $I_{dark}$ is the diode DC current in dark, and $J_n$ is the Bessel function of order $n$. The argument of the Bessel function ($qV_\omega/\hbar\omega$) determines the electron occupation probability of the $n$th state. At low solar intensities and high frequencies, only $n = -1, 0, 1$ have a significant contribution to the illuminated current.

### 3.2.2 Rectenna Circuit Model

The rectenna circuit consists of an antenna, a diode, and a parallel load connected through leads. As shown in Fig. 3.2, the antenna is represented by a high-frequency voltage source $V_S$, an impedance $R_S$, and a DC blocking capacitor $C$ to model the fact that DC current is blocked by the antenna. The diode is connected in series with the antenna. The load $R_L$ is in parallel with the diode, and the leads connecting the two are represented by a large inductance $L$, the role of which is to filter the output to a DC voltage. The circuit works as a voltage clamping circuit, and, as a result, the voltage across the diode consists of an alternating voltage ($V_\omega$) due to the source and a DC self-bias ($V_D$), which drops across the load. PAT is used to determine the current flowing through the diode under illumination. Alternating currents at multiple frequencies ($I_\omega$) flow through the source and diode circuit loop, while direct currents ($I_{illum}$) flow through the diode and the load. We assume that the diode capacitance is small so that any RC falloff of the alternating voltage across the diode is neglected.

For the purpose of finding efficiency limits, we model the rectenna as having ideal components. The antenna is modeled as a voltage source ($V_S$) connected to antenna impedance ($R_S$), which is assumed to be 100 Ω. $P_{in}$ is the input power to the rectenna. A perfectly matched load resistor connected across the antenna terminals would dissipate this power most effectively, so that $P_{in} = {V_S}^2/8R_S$. The relation $V_S = \sqrt{8P_{in}R_S}$ can be used to determine the source voltage produced by the antenna. The alternating voltage across the diode is calculated using the vector equation

$$\overline{V_\omega} = \overline{V_S} - \overline{I_\omega} R_S \tag{3.2}$$

The bar over the voltage and current terms denotes that they are vectors consisting of multiple frequency components. The alternating current $I_\omega$ is a function of the alternating voltage $V_\omega$, and we solve the equation self-consistently to reach a stable solution, as described in Sect. 3.3. A nonlinear diode will generate higher-order voltage and current harmonics, which makes the solution more complex.

### 3.2.3 *Diode* I(V) *Characteristics*

To study diode efficiency limits, we assume that the diode has negligible reverse leakage. When the diode is illuminated, its resistance is different from the DC resistance, as it is modified due to PAT and is a function of the photon energy. The resistance offered by the diode to a photon of energy $\hbar\omega$ is given by the reciprocal of the slope of the secant connecting the points on the diode $I(V)$ characteristics one $\hbar\omega/q$ higher and lower than $V_D$, as described in Sect. 2.2 [7]. The following equation, (3.3), gives the modified diode secant resistance $R_\omega$:

$$R_\omega = \frac{2 \times (\hbar\omega/q)}{I_{dark}(V_D + \hbar\omega/q) - I_{dark}(V_D - \hbar\omega/q)} \tag{3.3}$$

We choose the diode forward resistance at optical frequencies to match the antenna impedance for maximum power transfer to the diode. We can simplify (3.3) to obtain the condition for perfect matching under the assumption of negligible reverse bias current,

$$R_\omega \approx \frac{2 \times (\hbar\omega/q)}{I_{dark}(V_D + \hbar\omega/q)} = \frac{2 \times (\hbar\omega/q)}{m \times (-|V_D| + \hbar\omega/q) + b} \tag{3.4}$$

In the above equation, we take the dark $I(V)$ in the first quadrant as a straight line of the form $y = mx + b$, where $m$ is the slope and $b$ is the $y$-axis intercept. By inspection, for $m = 1/R_{DC}$ and $b = |V_D|/R_{DC}$, we obtain $R_\omega = 2R_{DC}$. The values of $m$ and $b$ are such that the diode impedance is independent of the photon energy $\hbar\omega$.

Thus, to perfectly match the antenna and the diode at a particular $V_D$, the required $I(V)$ is such that its first quadrant differential resistance $R_{DC}$ is half the antenna impedance and an extrapolation of the $I(V)$ intercepts on the $x$-axis at $V_D$, as shown in Fig. 3.3. In the analyses of efficiency limits that follow in Sect. 3.3, we have used $I(V)$ characteristics based on the same idea.

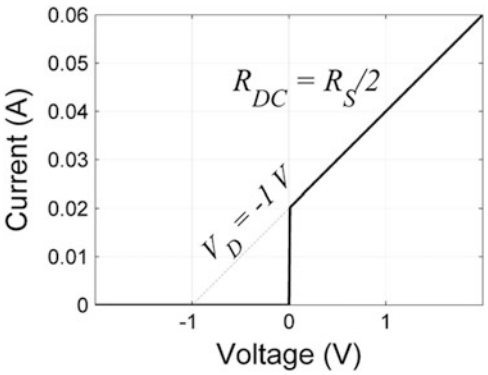


**Fig. 3.3** Diode current–voltage [$I(V)$] characteristics for optimum match with the antenna at optical frequencies, for a particular rectenna operating voltage ($V_D$) The reverse leakage current is assumed to be negligible. The slope of the $I(V)$ curve is the inverse of the DC diode resistance ($R_{DC}$), which is equal to half the source impedance ($R_S$). The $I(V)$ curve intercepts the $x$-axis at the rectenna operating voltage. This provides an optical frequency secant resistance that perfectly matches the antenna. A diode with a different intercept is used for each value of $V_D$

## 3.3 Efficiency Limits of Rectification

To determine the maximum rectenna efficiency, we choose a diode with negligible reverse leakage current and a forward resistance that matches the antenna and the diode for optimum power transfer, as explained in Sect. 3.2. In the sections that follow, we analyze rectenna efficiency limits for monochromatic, dichromatic, and broadband illumination.

To calculate the current through the diode in a rectenna circuit shown in Fig. 3.2, under single and multiple input frequencies, we have generalized the method discussed in Ref. [22]. In Fig. 3.4, we show a flowchart of the process that has been used. First, we determine the incident power on the device and the antenna source voltage $V_S(t)$ that would be required to transfer the incident power to a matched load resistor, refer 3.4a, b. At a particular rectenna DC self-bias operating voltage, we assume a time-domain alternating voltage $V(t)$ across the diode, 3.4c, which is used as a perturbation of the initial electronic states to calculate a phase factor $W(t)$, 3.4d. The phase factor is defined in (3.5)

$$W(t) = \exp\left[\frac{-iq}{\hbar}\int^{t} V(t')\mathrm{d}t'\right] \tag{3.5}$$

Diode illuminated current in the time domain (consisting of DC, fundamental, and higher harmonic components) is calculated, using the phase factor and the diode dark $I(V)$ characteristics using (3.6)

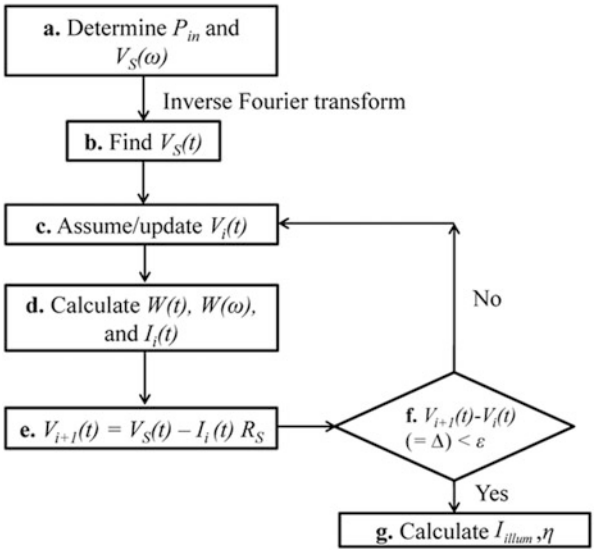


**Fig. 3.4** Flowchart of the method used to determine the diode illuminated current. (**a**) Calculate $P_{\text{in}}$ and determine the source voltage $V_{\text{S}}(\omega)$. (**b**) Perform an inverse Fourier transform to find $V_{\text{S}}(t)$. (**c**) Assume voltage $V(t)$ across the diode in a circuit. (**d**) Calculate the phase factor $W(t)$ and $W(\omega)$ and determine $I(t)$ using (3.6). (**e**) Apply KVL to find the voltage across the diode. (**f**) This value is compared to the initially assumed $V(t)$ to calculate the difference $\Delta$. If $\Delta$ is greater than some small number $\varepsilon$, the value of $V(t)$ is updated, and steps (**c**–**e**) are repeated. If $\Delta$ is less than $\varepsilon$, the latest $I(t)$ is used to calculate $I_{\text{illum}}$

$$\langle I(t)\rangle = \text{Im}\left[\int\int \text{d}\omega' W(\omega') j\left(\omega' + \frac{qV_{\text{D}}}{\hbar}\right)\text{e}^{-i\omega t} \times \text{d}\omega'' W*(\omega'')\text{e}^{i\omega'' t}\right] \tag{3.6}$$

Here, $j$ is the diode response function, the imaginary part of which is the diode DC dark $I(V)$ characteristics, $\omega$ is the frequency, and $W(\omega)$ is the Fourier transform of the phase factor. The expression is integrated over the range of incident frequencies to calculate the current. The flow of current in the source impedance modifies the voltage across the diode, 3.4e, as per Kirchhoff's voltage law (KVL). The difference in the assumed and modified diode voltage, denoted by $\Delta$, is compared to a small number $\varepsilon$. The last two steps are used iteratively to solve for the stable steady-state current through the diode which determines the diode DC illuminated current ($I_{\text{illum}}$) and efficiency $\eta$, 3.4g. A sequence of load-dependent DC operating voltages are used to determine the diode illuminated $I(V)$ characteristics. The rectified DC output power is the product of the direct current flowing in the load and the DC operating voltage across it. Rectenna efficiency is calculated as the ratio of the output DC power to the input AC power.

In the following subsections, we find that efficiencies up to 100 % can be obtained in the monochromatic case and decrease thereafter for the other cases, due to nonoptimal utilization of every photon to its maximum potential.

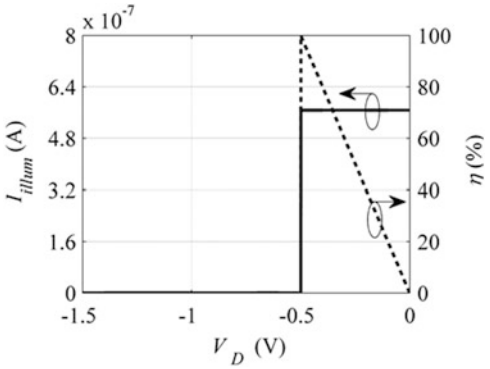


**Fig. 3.5** Illuminated $I(V)$ (*solid*) and efficiency characteristics (*dashed*) of a diode under monochromatic illumination. Photon energy is 0.5 eV. The input power is 283 nW, which is the power of one sun (1,000 W/m$^2$) over a device coherence area of 19 μm. The efficiency approaches 100 % as the rectenna operating voltage approaches −0.5 V, where the 0.5 eV photon is utilized most efficiently

### 3.3.1 Monochromatic Illumination

For the case of monochromatic illumination of the rectenna, we have assumed that the energy of the incoming photons is 0.5 eV and the input power is 283 nW, which is the power of one sun (1,000 W/m$^2$) over a device coherence area corresponding to a diameter of 19 μm. Above this area, the coherence in the power coupled to the antenna decreases, as described in Chap. 4. We choose the area such that the coherence efficiency is 97 % [23, 24]. For the case of single-frequency AC voltage across the diode, the alternating current ($I_\omega$) through the diode is given by (3.7)

$$I_\omega = \sum_{n=-\infty}^{\infty} J_n\left(\frac{qV_\omega}{\hbar\omega}\right) \times \left[J_{n+1}\left(\frac{qV_\omega}{\hbar\omega}\right) + J_{n-1}\left(\frac{qV_\omega}{\hbar\omega}\right)\right] \times I_{\text{dark}}\left(V_{\text{D}} + n\frac{\hbar\omega}{q}\right) \quad (3.7)$$

We use the general method outlined in the beginning of this section and (3.2) to calculate the illuminated DC current through the diode. The results are shown in Fig. 3.5. As the operating voltage increases beyond the photon energy, the illuminated DC current falls to zero. For an optimal diode, the efficiency of the rectenna under monochromatic illumination can approach 100 %. The illumination intensity is low so that only $n = -1$, 0, and 1 order Bessel terms are significant in contributing to the rectified current.

These results can be interpreted using the concept of a rectenna bandgap. In a rectenna under monochromatic illumination, optimal coupling to the diode transfers the power of the entire incident light to the diode. If the diode operating voltage is less than the photon energy (i.e., $|qV_{\text{D}}| < \hbar\omega$), photons can efficiently assist electrons to tunnel through the diode. In this quantum limit, at every operating voltage below the photon energy, each photon produces one electron of current, i.e.,

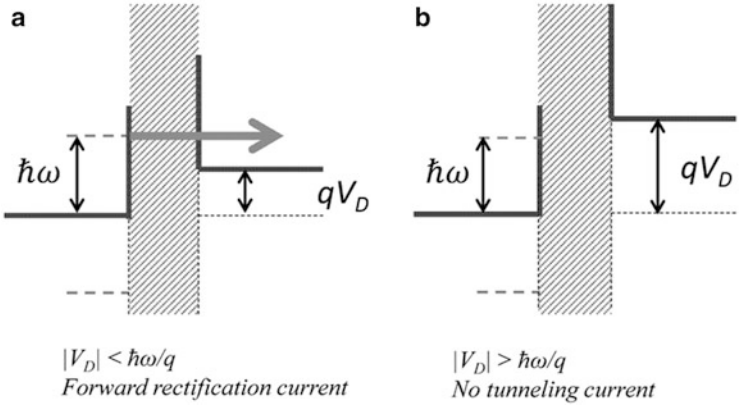


**Fig. 3.6** Illustration of PAT in a metal-barrier-metal diode when an AC field is incident on the rectenna. (**a**) Operating voltage ($qV_D$) less than the photon energy ($\hbar\omega$). Forward current flows in the diode allowing rectification of the incident field. (**b**) Operating voltage greater than the photon energy. The reverse leakage currents dominate and there is no forward tunneling. The *shaded* region represents a hypothetical barrier that allows electron flow in one direction

unity quantum efficiency. In this situation, we expect the diode illuminated $I(V)$ characteristics to be rectangular in shape. The current is constant at the value corresponding to the short circuit current ($I_{SC}$) at zero operating voltage. As $|qV_D| < \hbar\omega$, photons are giving only part of the potential to contribute to the efficiency. As the operating voltage approaches the photon energy, the efficiency approaches 100 %. This is illustrated in Fig. 3.6a. For $|qV_D| > \hbar\omega$, the current drops to zero as the bandgap is greater than the photon energy (shown in Fig. 3.6b). This is the open circuit voltage ($V_{OC}$) of the rectenna under low-intensity monochromatic illumination. From Fig. 3.5, we verify that the product of $V_{OC}I_{SC}$ is equal to the input power of 283 nW, consistent with solar cell characteristics. The illuminated current (for $0 < |V_D| < \hbar\omega/q$) can be written as,

$$I_{\text{illum}} = \frac{P_{\text{in}}}{\hbar\omega/q} \tag{3.8}$$

As the input power is increased, higher-order effects become important. When the input power is increased (hypothetically) to $10^4$ suns over the same coherence area as 19 μm, second- and third-order electron excitations also appear in the illuminated $I(V)$ characteristics. We observe a finite current below −0.5 V due to second-order excitations, as shown in Fig. 3.7. This is hypothetical because it is not possible to concentrate sunlight while maintaining a constant coherence area. As the input power is increased further or the incident frequency is reduced, the results approach the classical case, as described in Sect. 3.5.

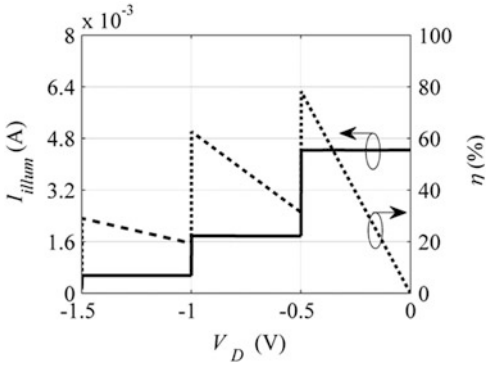


**Fig. 3.7** Illuminated $I(V)$ (*solid*) and efficiency characteristics (*dashed*) of a diode under monochromatic illumination. Photon energy is 0.5 eV. The input power is 2.83 mW, which is the power of $10^4$ suns over a device coherence area of 19 μm. At high intensities, higher-order effects appear in the illuminated $I(V)$ characteristics as some of the 0.5 eV photons combine to give second- and third-order electron excitations

### *3.3.2 Dichromatic Illumination*

For dichromatic illumination of the rectenna, the incident wave consists of coherent components at two different frequencies, $\omega_1$ and $\omega_2$. When the diode interacts with two frequencies, PAT theory predicts photon absorption and emission states at energy levels of $\hbar\omega_1$ and $\hbar\omega_2$ above and below the Fermi level in the metal. Alongside, mixing of photons gives rise to states at energy levels given by the sum and difference of the two photon energies and higher-order terms. These states are given by $\hbar(\omega_1 + \omega_2)$ and $\hbar(\omega_1 - \omega_2)$ as well as higher-order excitations and combinations of $\hbar\omega_1$ and $\hbar\omega_2$. At low intensities, the mixed and higher-order excitations are significantly smaller than the fundamental components and contribute to tunneling only at high-input intensities or low frequencies. The concept of mixing can be illustrated by developing the following simplified derivation of the current response under two-frequency illumination. The time-domain voltage across the diode is given as

$$V(t) = V_{\mathrm{D}} + V_1 \cos(\omega_1 t) + V_2 \cos(\omega_2 t) \tag{3.9}$$

$V_{\mathrm{D}}$ is the rectenna DC operating voltage; $V_1$ and $V_2$ are the voltage amplitudes of the alternating field at the frequencies $\omega_1$ and $\omega_2$ (for simplicity, assume $\omega_1 < \omega_2$). The alternating field affects the electron energy states near the Fermi level in the metal and gives rise to an additional phase factor. Following the perturbation approach of determining the diode response under illumination as in [21], we can calculate the phase factor as follows:

$$\begin{aligned} W(t) &= \exp\left[\frac{-iq}{\hbar}\int^{t}(V_1\cos(\omega_1 t\prime)+V_2\cos(\omega_2 t\prime))\mathrm{d}t\prime\right] \\ &= \exp\left[-i\frac{qV_1}{\hbar\omega_1}\sin(\omega_1 t)\right]\times\exp\left[-i\frac{qV_2}{\hbar\omega_2}\sin(\omega_2 t)\right] \\ &= \sum_{m=-\infty}^{\infty}J_m\left(\frac{qV_1}{\hbar\omega_1}\right)\exp[-im\omega_1 t]\times\sum_{n=-\infty}^{\infty}J_n\left(\frac{qV_2}{\hbar\omega_2}\right)\exp[-in\omega_2 t] \end{aligned} \tag{3.10}$$

Taking the Fourier transform of $W(t)$, we get

$$W(\omega\prime)=\sum_{m=-\infty}^{\infty}\sum_{n=-\infty}^{\infty}J_m\left(\frac{qV_1}{\hbar\omega_1}\right)J_n\left(\frac{qV_2}{\hbar\omega_2}\right)\times\delta(\omega\prime+m\omega_1+n\omega_2) \tag{3.11}$$

The average time-dependent diode current $\langle I(t)\rangle$ can be written as [21]

$$\langle I(t)\rangle=\mathrm{Im}\left[\int\int \mathrm{d}\omega\prime W(\omega\prime)j(\omega\prime+\frac{qV_\mathrm{D}}{\hbar})\mathrm{e}^{-i\omega\prime t}\times\mathrm{d}\omega\prime\prime W*(\omega\prime\prime)\mathrm{e}^{i\omega\prime\prime t}\right] \tag{3.12}$$

Here, $j$ is the diode response function, the imaginary part of which is the diode DC dark $I(V)$ characteristics. Simplifying further using (3.11) and (3.12) and performing a Fourier transform of the resulting time-domain expression, we obtain the DC component of the net current through the diode, which is also the rectified current due to illumination,

$$I_\mathrm{illum}=\sum_{m=-\infty}^{\infty}\sum_{n=-\infty}^{\infty}J_m^2\left(\frac{qV_1}{\hbar\omega_1}\right)\times J_n^2\left(\frac{qV_2}{\hbar\omega_2}\right)\times I_\mathrm{dark}\left(V_D+m\frac{\hbar\omega_1}{q}+n\frac{\hbar\omega_2}{q}\right) \tag{3.13}$$

In (3.13), $m$ and $n$ are integers and are the photon absorption and emission terms for photon energies $\hbar\omega_1$ and $\hbar\omega_2$.

The illuminated diode current and the efficiency of the rectenna under dichromatic illumination are shown in Fig. 3.8. The energies of the photons are 0.5 and 1.5 eV. The input power is 283 nW, which is the power of one sun (1,000 W/m$^2$) over a device coherence area of 19 μm. The ratio of the number of higher energy to lower energy photons is 1:3. The efficiency is lower than 100 % because at −0.5 V, only the 0.5 eV photons are utilized most efficiently. At operating voltages less than −0.5 V, the 0.5 eV photons do not contribute to the rectification current. Beyond −1.5 V, none of the photons contribute to the current. Since the input intensity is small, the contribution of the mixed and higher-order photons is negligible. This is understood from (3.13), which implies that at weak input intensities the occupation probability of the mixed and higher-order components is significantly less than the non-mixed components.

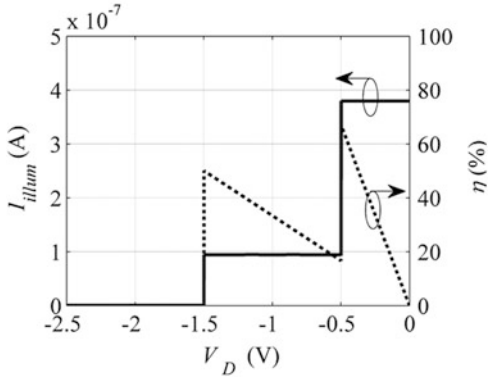


**Fig. 3.8** Illuminated $I(V)$ (*solid*) and efficiency characteristics (*dashed*) of a diode under dichromatic illumination. The energies of the photons are 0.5 and 1.5 eV. The input power is 283 nW, which is the power of one sun (1,000 W/m$^2$) over a device coherence area of 19 μm, as in Fig. 3.5. The ratio of the number of higher energy to lower energy photons is 1:3. 0.5 eV photons do not contribute to the current beyond an operating voltage of −0.5 V

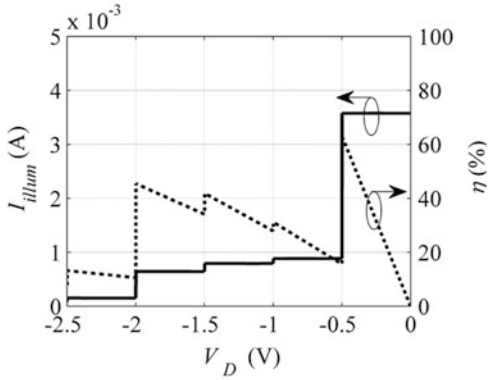


**Fig. 3.9** Illuminated $I(V)$ (*solid*) and efficiency characteristics (*dashed*) of a diode under dichromatic illumination. The energies of the photons are 0.5 and 1.5 eV. The input power is 2.83 mW, which is the power of $10^4$ suns over a device area of 19 μm. The ratio of the number of higher energy to lower energy photons is 1:3. At high-input intensities, 0.5 eV photons contribute to the current beyond the operating voltage of −0.5 V, and 1.5 eV photons contribute to current beyond −1.5 V due to mixing of 0.5 and 1.5 eV photons, as well as higher-order excitations

As shown in Fig. 3.9, increasing the input intensity to $10^4$ suns (2.83 mW), over a device area of 19 μm, shows the contribution of mixed and higher-order photons beyond operating voltages of −1.5 V. Using these photons at higher $|V_D|$ would be a way to use otherwise wasted low energy photons. In reality, however, rectennas cannot make use of a concentrated sunlight because of the coherence limitation, as concentration of different spatially coherent regions of the incident field would lead

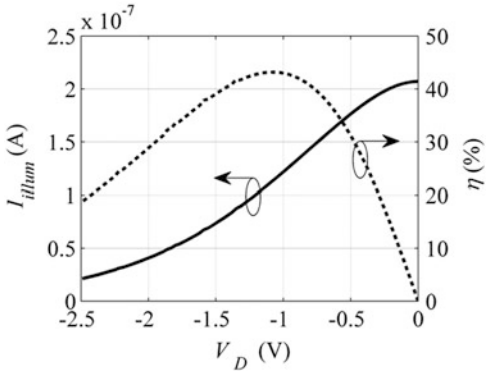


**Fig. 3.10** Illuminated $I(V)$ (*solid*) and efficiency characteristics (*dashed*) of a diode under broadband illumination. The input power is 283 nW, which is the power of one sun (1,000 W/m$^2$) over a device coherence area of 19 μm, as in Fig. 3.5. Efficiency peaks at ~44 % near the rectenna operating voltage of −1.1 V. Reprinted with permission [17]. Copyright 2013, American Institute of Physics

to cancellation of the fields. Improving the $I(V)$ characteristics would also increase the strength of the mixed and higher-order states, but at the cost of a poorer impedance match with the antenna.

### *3.3.3 Multispectral Illumination*

For illumination from the sun, the input intensity is low, and as in the Sects. 3.3.1 and 3.3.2, the input power is 283 nW, which is the power of one sun (1,000 W/m$^2$) over a device coherence area of 19 μm. We assume that the antenna is broadband. The method used to calculate the illuminated diode current for the broadband case is as follows. To approximate the sun, a temperature of 5,780 K for the blackbody source is used. This determines the shape of the intensity spectrum. The source voltage spectrum is given to have a shape approximated by the square root of the solar intensity spectrum. The amplitude of the source voltage spectrum is calculated such that the power dissipated in a matched load resistor is the same as the coherent power from the sun captured by the antenna. The time-dependent voltage waveform is determined using an inverse Fourier transform of this source voltage spectrum. Then we use (3.2) and (3.12) simultaneously to obtain the diode alternating voltage and the illuminated current, as discussed in the beginning of Sect. 3.3.

The diode illuminated current and rectenna efficiency plots are shown in Fig. 3.10. The efficiency approaches a maximum of 44 % at an operating voltage of 1.1 V, which is a result reminiscent of the Trivich-Flinn efficiency of solar energy conversion by quantum processes [25], later also proposed by Shockley and Queisser [4] as the ultimate efficiency of a solar cell made from a single junction.

When a rectenna is illuminated by a broadband frequency source, PAT leads to creation of multiple occupation states, but as a consequence of the low intensity, photon mixing is inefficient. At the operating voltage $V_D$, only photons having the energy $|qV_D|$ are used most efficiently. Photons having energy less than $|qV_D|$ are not used at all, while photons having energy greater than $|qV_D|$ are used in a partly efficient manner. This means that the operating voltage in rectenna solar cells plays the same role that bandgap plays in semiconductor p-n junction solar cells. It is possible to achieve higher efficiency limits if the spectrum is split into multiple portions and each portion of the spectrum is used by a rectenna operating at an optimum operating voltage, similar to multi-junction solar cells using materials having different bandgap. Nonideal diode $I(V)$ characteristics reduce the efficiency limit and are analyzed in the next section.

## 3.4 Nonideal Diodes

In this section, we analyze the effects of nonideal diode $I(V)$ characteristics. We will consider two types of diode imperfections:

(a) Diodes with $I(V)$ characteristics that are not matched to the antenna
(b) Diodes having finite reverse leakage currents

### *3.4.1 Diodes Not Matched to the Antenna*

In Sect. 3.3, we used diode $I(V)$ characteristics perfectly matched with the antenna impedance at each operating point, so that the incoming power was delivered to the diode with optimal efficiency. When the diode and the antenna are not matched to each other, the power coupling efficiency decreases. As a result, we expect the overall efficiency of the diode to decrease. In Fig. 3.11, we show the illuminated $I(V)$ and efficiency characteristics of a nonideal diode under monochromatic illumination having a finite forward DC resistance of 50 Ω and an infinite reverse resistance. In contrast to the ideal diode of Fig. 3.3, the $I(V)$ characteristics do not change with the operating voltage $V_D$. The energy of the incoming photons is 0.5 eV. The input power is 283 nW, which is the power of one sun (1,000 W/m$^2$) over a device coherence area corresponding to a diameter of 19 μm. The maximum efficiency approaches ~50 %. The current levels off due to increase in the resistance offered to the source by the diode as $|V_D|$ increases. Using (3.3), this increasing secant resistance for a 0.5 eV photon and a static diode $I(V)$ having a forward resistance of 50 Ω is plotted versus $V_D$ in Fig. 3.12. The diode resistance at optical frequencies increases and the matching becomes poor as $|V_D|$ is increased. The corresponding illuminated $I(V)$ characteristic and conversion efficiency for the solar broadband illumination case are shown in Fig. 3.13.

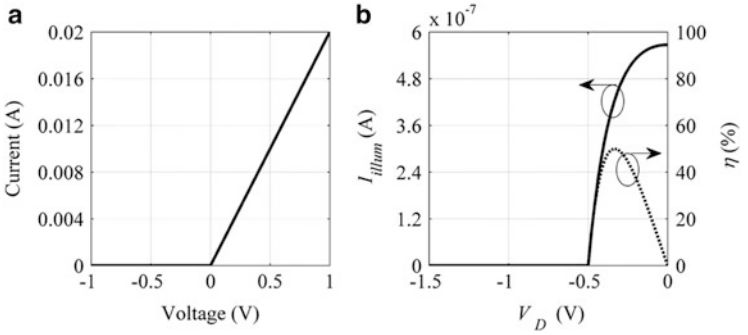


**Fig. 3.11** (**a**) Diode current–voltage [$I(V)$] characteristics for poor match with the antenna. The reverse leakage current is still assumed to be negligible. The slope of the $I(V)$ curve is the inverse of the DC diode resistance ($R_{DC}$) equal to 50 Ω, which is equal to half the source impedance ($R_S$). (**b**) Illuminated $I(V)$ (*solid*) and efficiency characteristics (*dashed*) of the poorly matched diode shown in (**a**) under monochromatic illumination. Photon energy is 0.5 eV. The input power is 283 nW, which is the power of one sun (1,000 W/m$^2$) over a device coherence area of 19 μm. The efficiency approaches a maximum of ~50 % at a $V_D$ of −0.35 V

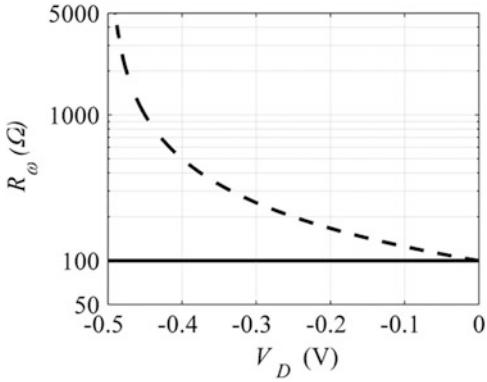


**Fig. 3.12** Plot of the optical frequency secant resistance offered by a diode, having a forward DC resistance of 50 Ω (*dashed*) and a matched diode (*solid*) shown in Fig. 3.3, to a photon having an energy of 0.5 eV versus the operating voltage $V_D$. The resistance mismatch between the antenna and the diode increases as $V_D$ is decreased

### 3.4.2 *Diodes with Finite Reverse Leakage Currents*

In Sect. 3.3, we considered diodes with zero reverse leakage current in the dark $I(V)$ characteristics. In this section, we consider the effects of diodes having a finite reverse resistance ($R_{rev}$). For the rectenna to operate efficiently, the reverse resistance must be high enough that the magnitude of the leakage current at the operating voltage is much lower than the photocurrent produced at a given illumination intensity. In Fig. 3.14, we show the illuminated $I(V)$ characteristics of a rectenna having a diode with a varying reverse resistance for monochromatic illumination with a photon energy of 0.5 eV. The input power is 283 nW, which is the power of one sun (1,000 W/m$^2$) over a device coherence area of 19 μm.

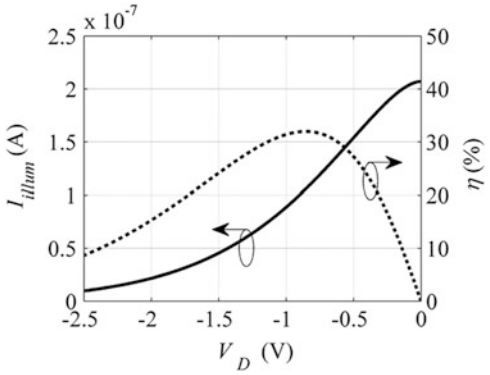


**Fig. 3.13** Illuminated $I(V)$ (*solid*) and efficiency characteristics (*dashed*) of a poorly matched diode under broadband illumination. The input power is 283 nW, which is the power of one sun (1,000 W/m$^2$) over a device coherence area of 19 μm, as in Fig. 3.5. The diode forward resistance is 50 Ω as in Fig. 3.11, so that the diode $I(V)$ characteristics are not optimized to match the antenna at different $V_D$. The maximum efficiency obtained is limited to ~32 %

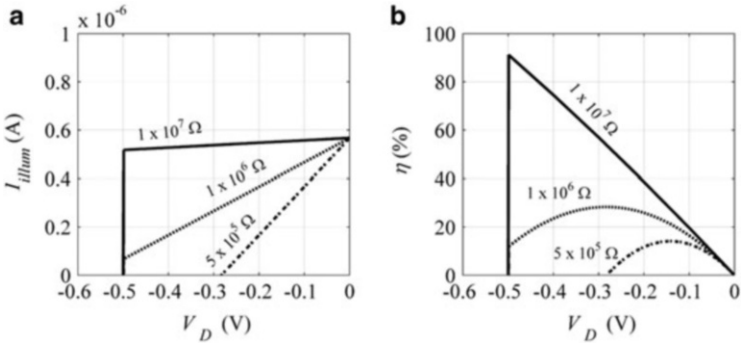


**Fig. 3.14** (**a**) Illuminated $I(V)$ and (**b**) efficiency characteristics of a diode under monochromatic illumination with varying diode reverse resistance and the ideal forward resistance shown in Fig. 3.3. Photon energy is 0.5 eV at an input power of 283 nW. The diode $I(V)$ has a reverse leakage resistance of $5 \times 10^5$ Ω (*dash-dot*), $10^6$ Ω (*dot*), and $10^7$ Ω (*solid*). The illuminated $I(V)$ characteristics change from being rectangular in shape to trapezoidal and triangular with the efficiency decreasing as the reverse leakage increases

The reverse resistance varies from $10^7$ Ω to $5 \times 10^5$ Ω. The forward diode $I(V)$ have the same characteristics as shown in Fig. 3.3 and change with the operating voltage. The illuminated $I(V)$ characteristics change from being rectangular in shape, as in Fig. 3.6, to trapezoidal, and finally approach a triangular form. The efficiency reduces from 100 % to a lower value that is a function of the leakage resistance.

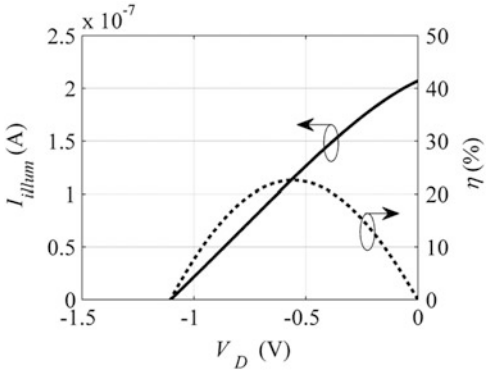


**Fig. 3.15** Illuminated $I(V)$ (*solid*) and efficiency (*dashed*) characteristics of a diode with a finite reverse resistance under broadband solar illumination. The input power is 283 nW, which is the power of one sun (1,000 W/m$^2$) over a device coherence area of 19 μm, as in Fig. 3.5. The diode $I(V)$ characteristics have a reverse leakage resistance of $10^7$ Ω. The forward diode characteristics are the same as those shown in Fig. 3.3. The maximum efficiency obtained is limited to ~22 %

The gradual decrease in the illuminated $I(V)$ from an operating voltage of 0 to −0.5 V is due to the leakage current. At low input intensities, the illuminated $I(V)$ characteristics are a strong function of the reverse bias leakage currents. This can be seen from the dependence of illuminated current on the $n = 0$ term of (3.1). Because the square of the Bessel term $J_O$ is close to 1, the reverse leakage current subtracts linearly from the constant current of Sect. 3.3.1. The dependence of the illuminated current on the operating voltage (for $0 < |V_D| < \hbar\omega/q$) is modified as,

$$I_{\text{illum}}(V_D) \cong \frac{P_{\text{in}}}{\hbar\omega/q} - \frac{|V_D|}{R_{\text{rev}}} \tag{3.14}$$

At $V_D = 0$ V, the above equation gives the expression for $I_{SC} = P_{\text{in}}/(\hbar\omega/q)$. As seen in Sect. 3.3.1, under low input intensities the maximum achievable $V_{OC}$ is $-\hbar\omega/q$ due to the bandgap of the rectenna. To ensure that $V_{OC} = -\hbar\omega/q$ requires that the photocurrent be larger than the leakage current at $V_{OC}$, i.e., $R_{\text{rev}} \geq (\hbar\omega/q)^2/P_{\text{in}}$. For the illumination conditions shown in Fig. 3.14, the shape of the $I(V)$ curve under illumination is trapezoidal if $R_{\text{rev}} \geq 0.88$ MΩ. For lower reverse resistances, the illuminated current has a triangular shape. An order of magnitude increase in $R_{\text{rev}}$ causes the operating regime to change drastically, leading to a sharp rise in efficiency. This reflects a critical balance between the reverse leakage and input power, in which the input power must provide a photocurrent that is much larger than the reverse leakage to maintain high efficiency.

In Fig. 3.15, we show the effect of having a reverse leakage resistance of $10^7$ Ω on broadband illuminated $I(V)$ characteristics. The maximum efficiency approaches 22 % which is below the ideal achievable rectenna efficiency of 44 %.

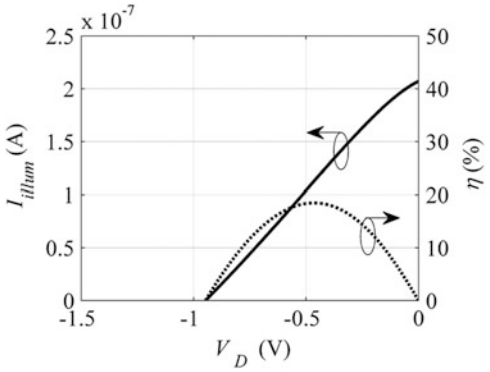


**Fig. 3.16** Illuminated $I(V)$ (*solid*) and efficiency characteristics (*dashed*) of a diode having a poor impedance match and a finite reverse leakage resistance under broadband solar illumination. The input power is 283 nW, which is the power of one sun (1,000 W/m$^2$) over a device coherence area of 19 μm, as in Fig. 3.5. As in Fig. 3.14, the diode $I(V)$ characteristics have a finite reverse leakage resistance of $10^7$ Ω. As in Fig. 3.11, the diode forward resistance is 50 Ω. The maximum efficiency obtained is limited to ~18 %

### *3.4.3 Diodes with Poor Impedance Match and Finite Reverse Leakage Currents*

In this section, we analyze diodes having the property of poor impedance matching with the antenna as in Sect. 3.4.1, in combination with a finite reverse leakage resistance, as in Sect. 3.4.2. This approaches the representation of a realistic rectenna. In Fig. 3.16, we show the illuminated $I(V)$ and efficiency characteristics of a device under broadband illumination from the sun. The diode reverse leakage resistance is $10^7$ Ω, and the forward resistance is a fixed 50 Ω independent of operating voltage $V_O$. The rectenna efficiency is low at ~18 %.

It is evident from Figs. 3.11, 3.12, 3.13, 3.14, 3.15, and 3.16 that the diode $I(V)$ characteristics are crucial for obtaining high-rectenna efficiency.

## 3.5 Classical Correspondence

In this section, we explain the correspondence between the classical and quantum theory of rectenna operation. In the limit of low frequencies (small $\hbar\omega/q$) and high intensities (large $V_\omega$), the results from the theory of PAT reduces to classical theory. The following derivation is an extension of that carried out for microwave rectification in Ref. [26]. For large $\alpha$ ($=qV_\omega/\hbar\omega$), the summation in (3.1) can be written in the form of an integral

$$I_{\text{illum}} = \int_{-\infty}^{\infty} J_n^2\left(\frac{qV_\omega}{\hbar\omega}\right) \times I_{\text{dark}}(V_{\text{D}} + n\frac{\hbar\omega}{q})\text{d}n$$

In general, for $n > \alpha$, the Bessel functions fall rapidly with $n$, and the limits of integration can be changed to

$$I_{\text{illum}} = \int_{-\alpha}^{\alpha} J_n^2(\alpha) \times I_{\text{dark}}\left(V_{\text{D}} + n\frac{V_\omega}{\alpha}\right)\text{d}n$$

Also, in the limit of large $\alpha$, the Bessel function can be reduced to an average value over a range of $n$,

$$I_{\text{illum}} = \int_{-\alpha}^{\alpha} \frac{1}{\pi\alpha\sqrt{1-\left(\frac{n}{\alpha}\right)^2}} \times I_{\text{dark}}\left(V_{\text{D}} + n\frac{V_\omega}{\alpha}\right)\text{d}n$$

Replacing $(n/\alpha)$ with $\beta$, we obtain

$$I_{\text{illum}} = \int_{-1}^{1} \frac{1}{\pi\sqrt{1-\beta^2}} \times I_{\text{dark}}(V_{\text{D}} + \beta V_\omega)\text{d}\beta$$

To obtain a simpler expression and a result familiar to the classical result, we substitute $\beta = \sin(\theta)$ to find

$$I_{\text{illum}} = \int_{-\pi/2}^{\pi/2} I_{\text{dark}}(V_{\text{D}} + V_\omega \sin\theta)\text{d}\theta \tag{3.15}$$

Following the same steps as above and using the identity $J_{n-1}(z) + J_{n+1}(z) = (2n/z)J_n(z)$, we can simplify (3.7) to obtain the alternating current in the diode

$$I_\omega = \sum_{n=-\infty}^{\infty} J_n(\alpha) \times \frac{2n}{\alpha} \times I_{\text{dark}}\left(V_{\text{D}} + n\frac{\hbar\omega}{q}\right) \tag{3.16}$$

In the limit of large $\alpha$ $(=qV_\omega/\hbar\omega)$, the summation in (3.16) can be written in the form of an integral

$$I_\omega = \int_{-\infty}^{\infty} \frac{2n}{\alpha} J_n^2(\alpha) \times I_{\text{dark}}\left(V_{\text{D}} + n\frac{\hbar\omega}{q}\right)\text{d}n$$

$$I_\omega = \int_{-\alpha}^{\alpha} \frac{2n}{\alpha} \times \frac{1}{\pi\alpha\sqrt{1-\left(\frac{n}{\alpha}\right)^2}} \times I_{\text{dark}}\left(V_{\text{D}} + n\frac{V_\omega}{\alpha}\right)\text{d}n$$

Replacing $(n/\alpha)$ with $\beta$, we obtain

$$I_\omega = \frac{2}{\pi}\int_{-1}^{1} \frac{\beta}{\sqrt{1-\beta^2}} \times I_{\text{dark}}(V_{\text{D}} + \beta V_\omega)\mathrm{d}\beta$$

To obtain a simpler expression and a result familiar to the classical result for the fundamental frequency component of the diode current, substitute $\beta = \sin(\theta)$, giving the following result:

$$I_\omega = \frac{2}{\pi}\int_{-\pi/2}^{\pi/2} I_{\text{dark}}(V_{\text{D}} + V_\omega \sin\theta) \times \sin\theta \times \mathrm{d}\theta \tag{3.17}$$

Similarly, using the above procedure, higher than fundamental frequency components can be shown to reduce to their classical forms. This shows that the classical case is an extension of the quantum case in the limit of large intensity and small photon energy. When $\hbar\omega/q$ is comparable to the diode DC $I(V)$ nonlinearity, nonlinear effects lead to a significant change in the physics, and classical analysis cannot be used to describe device operation. In this limit, the theory of PAT is used to explain diode behavior.

## 3.6 Conclusions

In this chapter, we studied the efficiency limits of rectenna solar cells. The rectenna is modeled as an equivalent circuit consisting of an antenna, a diode, and a load. The physics of PAT governs diode behavior in an optical rectenna and dictates principles behind the design of diodes for improving rectenna efficiency. To find the limiting efficiency, we chose ideal diode $I(V)$ characteristics for perfect power coupling between the antenna and diode. We showed that rectenna efficiency approaches 100 % for a diode under monochromatic illumination and 44 % for a diode under broadband solar illumination. Diode $I(V)$ characteristics limit rectenna efficiency and for high efficiency should provide a good impedance match with the antenna and have low reverse leakage currents. We also show the correspondence between the classical and quantum limits of rectification and conclude that in the limit of low intensity and $\hbar\omega/q$ comparable to the diode DC $I(V)$ nonlinearity, quantum analysis is required to describe device operation.

## References

1. Brown WC. Adapting microwave techniques to help solve future energy problems. IEEE Trans Microw Theory Tech. 1973;21:753–63.
2. Bailey RL. Proposed new concept for a solar-energy converter. J Eng Power. 1972;94:73–7.

3. Small JG, Elchinger GM, Javan A, Sanchez A, Bachner FJ, Smythe DL. AC electron tunneling at infrared frequencies: thin-film M-O-M diode structure with broad-band characteristics. Appl Phys Lett. 1974;24:275–9.
4. Shockley W, Queisser HJ. Detailed balance limit of efficiency of p-n junction solar cells. J Appl Phys. 1961;32:510–9.
5. McSpadden JO, Fan L, Chang K. Design and experiments of a high-conversion-efficiency 5.8-Ghz rectenna. IEEE Trans Microw Theory Tech. 1998;46:2053–60.
6. Landsberg PT, Tonge G. Thermodynamics of the conversion of diluted radiation. J Phys A Math Gen. 1979;12:551–62.
7. Grover S, Moddel G. Applicability of metal/insulator/metal (MIM) diodes to solar rectennas. IEEE J Photovoltaics. 2011;1:78–83.
8. Eliasson BJ. Metal-insulator-metal diodes for solar energy conversion. Ph.D. Thesis, University of Colorado; 2001.
9. Berland B. Subcontractor report. National Renewable Energy Laboratory. Subcontractor Report 2003; NREL/SR-520-33263.
10. Grover S, Moddel G. Engineering the current–voltage characteristics of metal–insulator–metal diodes using double-insulator tunnel barriers. Solid State Electron. 2012;67:94–9.
11. Miskovsky NM, Cutler PH, Mayer A, Weiss BL, Willis B, Sullivan TE, Lerner PB. Nanoscale devices for rectification of high frequency radiation from the infrared through the visible: a new approach. J Nanotechnol. 2012;2012:1–19.
12. Grover S, Dmitriyeva O, Estes MJ, Moddel G. Traveling-wave metal/insulator/metal diodes for improved infrared bandwidth and efficiency of antenna-coupled rectifiers. IEEE Trans Nanotechnol. 2010;9:716–22.
13. Moddel G, Zhu Z, Grover S, Joshi S. Ultrahigh speed graphene diode with reversible polarity. Solid State Commun. 2012;152:1842–5.
14. Sokolov IM. On the energetics of a nonlinear system rectifying thermal fluctuations. Europhys Lett. 1998;44:278–83.
15. Sanchez A, Davis CF, Liu KC, Javan A. The MOM tunneling diode: theoretical estimate of its performance at microwave and infrared frequencies. J Appl Phys. 1978;49:5270–7.
16. Corkish R, Green M, Puzzer T. Solar energy collection by antennas. Sol Energy. 2002;73:395–401.
17. Joshi S, Moddel G. Efficiency limits of rectenna solar cells: theory of broadband photon-assisted tunneling. Appl Phys Lett. 2013;102:083901.
18. Grover S, Joshi S, Moddel G. Quantum theory of operation for rectenna solar cells. J Phys D Appl Phys. 2013;46:135106.
19. Tien PK, Gordon JP. Multiphoton process observed in the interaction of microwave fields with the tunneling between superconductor films. Phys Rev. 1963;129:647–51.
20. Dayem AH, Martin RJ. Quantum interaction of microwave radiation with tunneling between superconductors. Phys Rev Lett. 1962;8:246–8.
21. Tucker JR, Feldman MJ. Quantum detection at millimeter wavelengths. Rev Mod Phys. 1985;57:1055–113.
22. Tucker J. Quantum limited detection in tunnel junction mixers. IEEE J Quantum Electron. 1979;15:1234–58.
23. Grover S. Diodes for optical rectennas. Ph.D. Thesis, University of Colorado; 2011.
24. Mashaal H, Gordon JM. Fundamental bounds for antenna harvesting of sunlight. Opt Lett. 2011;36:900–2.
25. Trivich D, Flinn PA. Maximum efficiency of solar energy conversion by quantum processes. In: Daniels F, Duffie JA, editors. Solar energy research. Madison: The University of Wisconsin Press; 1955.
26. Hamilton CA, Shapiro S. RF-induced effects in superconducting tunnel junctions. Phys Rev B. 1970;2:4494–503.